



Effect of structural parameters of peptides on dimer formation and highly oxidized side products in the oxidation of thiols of linear analogues of human β -defensin 3 by DMSO

Shouping Liu,^a Lei Zhou,^{a,b} Liyan Chen,^a Shubhra Ghosh Dastidar,^c Chandra Verma,^c Jing LI,^{a,b} Donald Tan^{a,b,d} and Roger Beuerman^{a,b*}

The purpose of this study was to examine the effects of structural parameters of peptides on their oxidation by DMSO, including location of cysteine, effect of adjunct group participation, molecular hydrophobicity, steric hindrance or the accessibility of thiol group and peptide conformation, on oxidation rates, dimer formation and associated side products. We designed and synthesized two series of linear cysteine-containing analogues of human β -defensin 3 (the C1-peptides with cysteine at the *N*-terminus residue 1, the C29-peptides with cysteine located at residue 29 in the centre of peptide), which were used for preparation of disulphide-linked homodimers. HPLC–ESI–MS was used to monitor the oxidation process and to characterize the molecular weights of dimers and side products of high oxidation. The formations of dimers and side products were dependent on the position of cysteines. Hydrophobicity generally rendered the thiol groups less accessible and hence exposed them to slow oxidation to form dimers (or even fail to form dimers during the timescale of observation). Molecular dynamics simulations showed that the exposure of cysteines (and sulphurs) of the C1-peptides was much larger than for the C29-peptides. The larger hydrophobic side chains tended to enable clustering of the side chains that sequester cysteine, particularly in the C29-peptides, which provided a molecular explanation for the observed trends in oxidation rates. Together with molecular modelling, we propose a reaction mechanism to elucidate the oxidation results of these peptides. Copyright © 2008 European Peptide Society and John Wiley & Sons, Ltd.

Supporting information may be found in the online version of this article

Keywords: human β -defensin 3 (hBD3); antimicrobial peptides; dimers; highly oxidized side products; DMSO; molecular hydrophobicity; molecular modelling

Introduction

Defensins are small, 3–5 kDa endogenous cationic peptides constrained by three disulfide bonds, and known for their broad-spectrum antimicrobial activity against Gram positive and Gram negative bacteria, fungi, and enveloped viruses and also against bacteria that have demonstrated resistance to the currently used antibiotics [1]. They are a critical part of the innate immune system that provides an initial antimicrobial barrier for mucosal surfaces such as the surface of the eye, airways, lungs and skin [2–6]. Because of this ability, they have come to be known as ‘natural antibiotics’. Interest in the defensins has also been aided by an increase in bacterial strains with resistance to the standard antibiotics and an increase in populations with reduced immunity. Moreover, their water solubility makes them potentially rapidly deployable in response to a pathogen release into the environment [7].

Defensins are classified into four families depending on the pattern of disulfide connectivities and are termed α -, β -, θ - and insect defensins. Among the human β -defensins, human β -defensin 3 (hBD3) has been of particular interest as it appears to possess the most potent broad-spectrum antimicrobial activity [8]. Additionally, hBD3 has significant bactericidal activity against

multidrug-resistant *Staphylococcus aureus* at physiological salt concentrations [9]. This has been attributed to the ability of wild type (wt) hBD3 to form noncovalent dimers and oligomers that are thought to have higher activity [9–13]. The dimerization is mediated across strand β 2 through an intermolecular hydrogen bond and two pairs of symmetric intermolecular salt bridges between Glu28 and Lys32 [9]. However, the noncovalent hBD3 dimer is stable only at high concentrations. Their chemical

* Correspondence to: Roger Beuerman, Singapore Eye Research Institute, 11 Third Hospital Avenue, #06-00, 16875, Singapore. E-mail: rwbeur@mac.com

a Singapore Eye Research Institute, 11 Third Hospital Avenue, Singapore 16875, Singapore

b Department of Ophthalmology, Yong Loo Lin School of Medicine, National University of Singapore, Singapore 119047, Singapore

c Bioinformatics Institute (A-STAR), 30 Biopolis Way, #07-01 Matrix, Singapore 138671, Singapore

d Singapore National Eye Center, 11 Third Hospital Avenue, Singapore 16875, Singapore

composition makes them amphiphilic, that is, they are both highly water soluble and can interact with the lipid environments of the cellular membranes. They are all highly positively charged together with a hydrophobic component, and it is believed that their cationicity enables them to be attracted to negatively charged surfaces of membranes while the hydrophobic residues insert into the hydrophobic membranes, thus leading to their membranolytic properties. Of course, this also makes them potentially toxic to human cells and hence the need to understand the molecular basis of such interactions towards the design of new and better peptides [14]. In addition, there are other unresolved issues such as resistance to proteolytic degradation, stable serum half-life and scaled production [15] and emergence of resistance [16]. This clearly suggests that although there is cause for an optimistic future for defensins, much more work needs to be done before a viable therapeutic is clinically available.

There is no clear picture as yet of comprehensive structure–function relationships in defensins. For example, the exact combination of cationicity and hydrophobicity that lends defensins their membranolytic characteristics remains unknown. Again, although the presence of intramolecular disulfide bonds seems to be required for maintaining the antimicrobial activity of human β -defensin 2 (hBD2) [13], neither their presence nor their position seems to have any significant influence on the antibacterial effects of hBD3 analogues [17–20]. Hence, we decided to exploit this property of hBD3 to construct variants that lack disulphide bridges, retain the overall cationicity and vary in hydrophobicity (cationicity was left unperturbed because it is thought to be the origin of the electrostatic force that drives defensins to accumulate at the negatively charged bacterial membrane surfaces).

The goal of the current study was to build on the above observations that hBD3 analogues are antimicrobial even in the absence of disulphide bridges and design mutants of homodimers of full-length linear analogues of hBD3 that were expected to have potentially higher antimicrobial properties (and hopefully display reduced toxicity to mammalian cells). The idea that dimers would have enhanced potency was based on observations of a synergistic increase in cationicity upon dimerization [10]. These homodimers were constructed by mutating out all the cysteines and replacing either residue 1 or 29 with cysteine which was then allowed to form a disulphide bridge with the corresponding cysteine in the other monomer. Similar experiments were carried out for position 46 and the data will be presented elsewhere. During this process, the net positive charge (+11) of the monomers was conserved, whereas the hydrophobicity was varied by replacing the six cysteine residues with Ala, Tyr and Trp. For the synthesis of peptides with intra- or intermolecular disulfide bonds, the formation of the disulfide bonds is often the final step, oxidized by common oxidation agents (e.g. iodine, ferric chloride, hydrogen peroxide and air) and DMSO [21–23]. However, there are associated problems such as the formation of complex mixtures of dimeric isoforms with as yet unknown inter- and intramolecular disulfide connectivities [12] and higher oxidation side products and the additional difficulty of separation of such a complex mixture [12,17,22].

In this endeavour, we have successfully synthesized a set of linear analogues of defensins with good antimicrobial properties and reduced cytotoxicity to mammalian cells [20]. Here, we have systemically examined the effects of structural parameters including variations in sequence, location of the cysteine residue, adjunct group (NH₂) participation, molecular hydrophobicity,

steric factors (the accessibility of the thiol group) and peptide conformation on the oxidation of these peptides. We examined the formation of dimers of variants of two series of linear analogues of hBD3. In the synthesis of the two series of 45-residue analogues of hBD3 (Scheme 1), we have systematically replaced the six original cysteine residues with Ala, Tyr and Trp; we then replaced either residue 1 (Gly) with cysteine (Series 1, the C1-peptides) or residue 29 (Gln) with a cysteine (Series 2, the C29-peptides). This unique cysteine is the site of oxidation and subsequently the homodimer is formed via a disulphide linkage through this cysteine side chain.

Materials and Methods

SPSS of Cysteine-containing Linear Analogues of hBD3 and Characterization

Fmoc-protected L-amino acids and resin were purchased from Advanced ChemTech (now Advanced Automated Peptide Protein Technologies, aappTEC; Louisville, KY, USA) and were used with the following side-chain protective groups: Arg(pbf), Lys(Boc), Tyr(But), Trp(Boc), Thr(But), Ser(But), Gln(Trt), Glu(OBut), Asn(Trt), Cys(Trt), and Fmoc-Lys(Boc)–Wang resin (substitution 0.72 mmol/g). Syntheses of two series of linear cysteine-containing analogues of hBD3, in which the cysteine is located at either the *N*-terminus (residue 1) or in the middle of the peptide (residue 29), respectively, were carried out on an Apex 396 by Fmoc chemistry. Peptides were coded as C1A6, C1Y6, C1W6, C29A6, C29Y6 and C29W6. Acylation (coupling reaction) was carried out with HBTU–HOBT in DMF at a synthesis scale of 0.04 mmol. Fmoc deprotection was carried out with 20% piperidine in DMF. The resulting peptidyl resins were treated with a freshly prepared mixture of TFA/TIS/phenol/thioanisole/water (90/1/2.5/5/1.5, the ratio of volume percent) for 2–3 h at room temperature. The crude peptides were then precipitated by filtration into ice-cold diethyl ether, separated by centrifugation, washed 3 times with ice-cold diethyl ether and dried by automated evaporation of ether and other remaining or residual solvents in crude solid products in a fume hood or dried under vacuum at room temperature. For further purification, the crude products were dissolved into mixtures of solvents (5% acetonitrile (ACN), 0.1% TFA in H₂O), and loaded onto a semi-preparative column (Delta PAK C18, 300 × 7.8 mm I.D., 15 μ m, 100 Å, Waters, Milford, MA, USA) at flow rate 3 ml/min; eluent A, 0.01% TFA in deionised water; eluent B, 0.01% TFA in ACN; gradient 20–35% of eluent B in 20 min; UV detection at 210 nm (Waters 2695 separation module with an autosampler and 996 photodiode array detector). Purified peptides were characterized by analytical HPLC–ESI–MS coupled system (Microass Platform LCZ, Waters Associates using a Delta PAK C18, 150 × 3.9 mm I.D., 5 μ m, 100 Å) at flow rate 0.2 ml/min; gradient 20–36% of eluent B in 20 min.

The Oxidation of Linear Analogues of hBD3 by DMSO

The required amount of freeze dried fractions of purified peptide monomers (C1A6, C1Y6, C1W6, C29A6, C29Y6 and C29W6) were dissolved in 150 μ l of 6 M guanidine hydrochloride. A small volume (e.g. 5 μ l) of 2 M ammonium acetate was used to adjust the pH of the solution to around 6.5. A small volume of 20% DMSO in 0.1 M Tris–hydrochloride (Tris–HCl) (5 μ l) was added, and the solution was placed in an automated shaker. HPLC–ESI–MS was used to monitor and determine the oxidation process, analyze and characterize the oxidation products.

Molecular Dynamics Simulations

To examine the conformations of the peptides in their folded states and the effects these may have on dimerization, we carried out molecular dynamics simulations of the monomeric forms of the peptides. The initial structures of the peptides were generated in their extended forms by using the modelling package QUANTA (Accelrys Inc, San Diego, CA, USA). Simulations were performed using the AMBER package utilizing the AMBER-ff03 force field [24]. After energy minimization, all atom molecular dynamics simulations were run using the Generalized Born (GB) [25,26] model to mimic the solvent water. The dielectric constants of the protein interior and solvent were set to 1 and 78.5, respectively. Non-bonded cut-off was set to 12 Å. SHAKE was applied to constrain the vibration of the bonds involving hydrogen atoms for computational efficiency [27]. All simulations were carried out at a constant temperature of 300 K, maintained by coupling to a Berendsen thermostat [28]. Each of the six peptides was simulated for 25 ns, totalling 150 ns in all.

Results and Discussion

Synthesis of Cysteine-containing Linear Analogues of hBD3

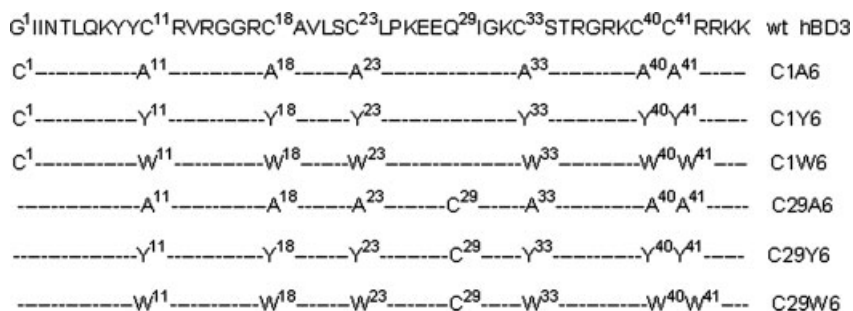
We have designed, synthesized and purified two series of model peptides (C1-peptides: C1A6, C1Y6 and C1W6; C29-peptides: C29A6, C29Y6 and C29W6) as monomers that were subsequently oxidized to form their corresponding homodimers by DMSO. The sequences of wt hBD3 and the two series of cysteine-containing linear full-length analogues of hBD3 are shown in Scheme 1.

The solid-phase synthesis of the six linear analogues of hBD3 with 45 residues and the same net positive charge (+11) was

performed using Fmoc chemistry. The purification of the six monomers were carried out and measured on a semi-preparative RP C18 HPLC column. The purity of the six analogues were measured on analytical RP C18 HPLC column and was based on area percentage of UV peak at 210 nm at 0 h without adding DMSO (Table 1). The spectrum of the six analogues confirmed that pure linear analogues with free thiol groups were obtained. The RP-HPLC–UV chromatogram and MS spectrum of the six monomers are provided in Figures 1–6 in the Supporting Information. Of the six analogues, five analogues had high purity (92–100%), whereas C1A6 was isolated with a purity of 73%.

Molecular Hydrophobicity Analysis Via RP-HPLC and Modelling

We have measured the molecular hydrophobicity by RP-HPLC in terms of retention time (Rt, min) and ACN% of UV peak with the experiments carried out on semi-preparative RP C18 HPLC column (Table 1). RP-HPLC is an approach that is commonly used for comparisons of peptides or amino acid side chains among antibacterial peptides [20,29–33]. Because the stationary phase of C18-modified silica is hydrophobic and the mobile phase (water–acetonitrile) is hydrophilic, a longer retention time is a measure of greater hydrophobicity if the same HPLC profile is applied. As the HPLC profile equations (ACN%) for the six analogues were somewhat different, the comparison of retention times was not accurate, hence we compare ACN% of UV peak; greater ACN% is a measure of greater hydrophobicity. The measured order for the relative molecular hydrophobicity of the six monomers was as follows: C1A6 < C29A6 < C1Y6 < C29Y6 < C1W6 < C29W6. This order also showed that each C29-peptide was



Scheme 1. Sequences of the C1-peptides and the C29-peptides.

Table 1. Molecular hydrophobicity of monomers measured by semi-preparative HPLC column in terms of retention time (Rt, min) and ACN% of UV peak, theoretical calculation and purity of monomers

Analogue	Retention time of UV peak	ACN% of UV peak ^a	Hydrophobicity ^b (least to most)	Purity (%) ^c	HPLC profile equation ACN (%)
C1A6	11.04 ± 0.09	26.42 ± 0.04	−5.5	73	22 + 0.40 × Rt
C29A6	13.39 ± 0.08	27.36 ± 0.03	−25.7	100	22 + 0.40 × Rt
C1Y6	12.36 ± 0.18	28.18 ± 0.09	−33.3	92	22 + 0.50 × Rt
C29Y6	11.73 ± 0.26	28.40 ± 0.09	−33.5	100	24 + 0.38 × Rt
C1W6	9.24 ± 0.08	30.70 ± 0.03	−39.9	100	27 + 0.40 × Rt
C29W6	13.85 ± 0.12	30.46 ± 0.03	−40.1	100	27 + 0.25 × Rt

^a Based on the average of five runs on semi-preparative column.

^b The Hopp–Woods scale was 'normalized' by excluding the values for polar-charged residues in all cases.

^c Purity was based on area percentage of UV peak at 210 nm at 0 h without adding DMSO.

Table 2. Molecular hydrophobicity of monomers and oxidation products measured by analytic HPLC column in terms of retention time (Rt, min) and ACN% of UV peak, theoretical calculation

Analogue	Retention time of UV peak	ACN% of UV peak ^a	Hydrophobicity ^b (least to most)	HPLC profile equation ACN (%)
C1A6	13.38 ± 0.69	27.35 ± 0.27	-25.5	22 + 0.40 × Rt
C29A6	17.48 ± 0.64	28.97 ± 0.03	-25.7	22 + 0.40 × Rt
Side product 1 of C1A6	17.86 ± 0.11	29.15 ± 0.04	NA	22 + 0.40 × Rt
C1Y6	16.61 ± 0.07	30.30 ± 0.03	-33.3	22 + 0.50 × Rt
C29Y6	15.46 ± 0.24	28.64 ± 0.07	-33.5	24 + 0.30 × Rt
Side product 1 of C1Y6	19.15 ± 0.15	31.57 ± 0.07	NA	22 + 0.50 × Rt
C1W6	11.73 ± 0.32	31.96 ± 0.12	-39.9	28 + 0.40 × Rt
C29W6	16.24 ± 0.17	33.50 ± 0.06	-40.1	27 + 0.44 × Rt
Side product 1 of C1W6	16.50 ± 0.16	33.65 ± 0.07	NA	28 + 0.40 × Rt
C1A6-dimer	20.41 ± 0.13	30.16 ± 0.05	-51	22 + 0.40 × Rt
C29A6-dimer	24.26 ± 0.36	31.71 ± 0.08	-51.4	22 + 0.40 × Rt
C1Y6-dimer	21.20 ± 0.15	32.60 ± 0.07	-66.6	22 + 0.50 × Rt
C29Y6-dimer	NA	NA	-67	24 + 0.30 × Rt
C1W6-dimer	20.38 ± 0.43	35.23 ± 0.17	-79.8	28 + 0.40 × Rt
C29W6-dimer	NA	NA	-80.2	27 + 0.44 × Rt

^a Based on the average of three runs on analytic column.^b The Hopp–Woods scale was 'normalized' by excluding the values for polar-charged residues in all cases.

more hydrophobic than the corresponding C1-peptide (Tables 1 and 2).

The relative hydrophobicities of the peptides were also calculated based on the Hopp–Woods hydrophilicity scale [34] (Tables 1 and 2). The general trend in computed hydrophobicity of the peptides using this scale generally matched that of the experimental HPLC ACN% data and partially matched that of retention time data (the reason for partial matching is due to some differences in the HPLC profiles).

The Oxidation of *N*-terminus Cysteine-containing Defensin Analogues (The C1-peptides, C1A6, C1Y6 and C1W6) by DMSO

We have systemically examined the percentage change of monomers, the primary oxidation products (dimers), and the side products of the *N*-terminus cysteine-containing peptides (C1-peptides, C1A6, C1Y6 and C1W6) in the presence of DMSO at room temperature. Table 3 shows the oxidation results of C1A6

by DMSO. We observed that C1A6 was already partially oxidized yielding C1A6-dimer (25%) and two side products (2%) by air during purification and storage (0 h). The complete oxidation of C1A6 was finished some time between 8 and 24 h. We observed C1A6-dimer as the major product (96%) after 24-h oxidation and remainder as minor side products in higher oxidation states: product 1 (sulfenic acid, *R*-SOH) and product 2 (sulfinic acid, *R*-SO₂H). The RP-HPLC–UV chromatogram and total ion current (TIC) spectrum of the oxidation of C1A6 at 1 h are shown in Figure 1(a), (b), whereas the ESI–MS analysis and the deconvoluted MS spectrum in ESI–MS analysis of C1A6 monomer, C1A6-dimer and the two side products are shown in Figure 1(c), (d), (e), (f), (g), (h), (i) and (j), respectively. Table 2 shows the retention time, ACN% of UV peak, the hydrophobicity of the various species. For the oxidation of C1A6 and C29A6, as the same HPLC profile was applied, the order for retention time and ACN% was the same, which generally matched that calculated. The order was as follows: C1A6 < C29A6 < side product 1 of C1A6 < [side product

Table 3. The oxidation results of C1A6 by DMSO

Oxidation time (h)	Percentage of monomer	Percentage of dimer	Percentage of side product 1	Percentage of side product 2
0	73	25	1	1
1	31	61	6	2
2	26	68	5	0
3	14	81	5	0, but traces observed by MS
4	5	91	4	0, but traces observed by MS
8	4	91	4	0, but traces observed by MS
24	0	96	4	0

The oxidation concentration of peptide C1A6 was 3.1 mg/ml. At 1 h of oxidation, monomer (MW: 5014.9, theory; 5017.0, experiment); dimer: *R*-S-S-*R*, (MW: 10027.9, theory; 10033.0, experiment); side product 1, sulfenic acid (*R*-SOH), (MW: 5030.9, theory; 5029.0, experiment); side product 2, sulfinic acid (*R*-SO₂H), (MW: 5046.9, theory; 5042.0, experiment).

Percentage was based on UV peak area at 210 nm; sometimes some oxidation side products were <1% and were reported at 0 h without adding DMSO but with trace in MS. Percentage was just a rough estimate as the peaks were at times small or noisy, making it difficult to integrate.

2, see Figure 1(a), (b)] < C1A6-dimer < C29A6-dimer. The general order for hydrophobicity of the various species measured by HPLC generally matched the calculated values and was as follows: C1-peptide monomer < C29-peptide monomer < side product 1 of C1-peptide < side product 2 of C1-peptide < C1-peptide-dimer < C29-peptide-dimer (the data pertaining to side product 2 of C1-peptide is not shown in Table 2, as its amount was very minor often 0–2%; this product often locates at the left shoulder peak of the C1-peptide-dimer, just like the oxidation of C1A6 (shown in Table 2 and Figure 1(a), (b)).

Table 4 shows the oxidation of C1Y6 by DMSO. In the first trial of oxidation, it was also observed that C1Y6 monomer (92%) had partially been oxidized to two side products of C1Y6 (5% and 3%, respectively) by air during purification and storage even before the addition of DMSO (0 h), yielding small amounts (total amount of 8%) of the two side products. Despite this, it was still very clear that the oxidation products of C1Y6 by DMSO were similar to that of C1A6. The amount of C1Y6-dimer obviously increased with time; however, the oxidation of C1Y6 seemed a little slower than that of C1A6. It was observed that C1Y6-dimer (84%) plus side product 1 (8%) of C1Y6 were formed; meanwhile, the C1Y6 monomer was still present (8%) after 5 days of oxidation. The reason for the slow oxidation rate could be due to the higher hydrophobicity of C1Y6 in comparison with C1A6.

A second attempt was made with efforts to avoid the interruption of partial oxidation of C1Y6 by air and the results are shown in Table 1SI (see Supporting Information). Although there was no initial oxidation by air, the second trial of oxidation yielded results similar to that of the first attempt: 88% of C1Y6-dimer and 12% of the side product 1.

The oxidation results of C1A6 and C1Y6 mentioned above showed that DMSO was a mild and suitable oxidation agent to

prepare their corresponding homodimers as major products. The dimers were easily purified as the amount of the side product 2 was small (0–2%), whereas the amount of the side product 1 was 4–12%. Furthermore, there was enough retention time gap between dimer and side product 1 (~2 min).

Effect of molecular hydrophobicity.

The oxidation results of C1W6 are shown in Table 5. It was observed that the percentage of the C1W6-dimer gradually increased with time. After 48 h of oxidation, the C1W6-dimer was the major product (54%) and the side product 1 was minor (4%). This result also showed that the rate of oxidation of C1W6 by DMSO was lower than that of C1A6 and C1Y6. For example, after 24 h of oxidation time, 75% of C1W6-monomer was still observed; however, no C1A6 (0% at 24 h, Table 3) and C1Y6 (0% at 24 h, the second trial, Table 1SI in Supporting Information); small amounts of C1Y6 (27% at 24 h, the first trial, Table 4) were observed indicating that the oxidation progress of C1W6 had not yet reached completion. The reason for the slower oxidation rate of C1W6 may be due to its highest hydrophobicity among the C1-peptides (Tables 1 and 2), which makes the accessibility of cysteine in C1W6 the lowest among the C1-peptides upon the folding of these peptides as shown in Figure 4.

Lowé has reported the oxidation of thiols of small organic molecules and a series of oxidation products from disulfides ($R-S-S-R$) to sulfonic acids ($R-SO_3H$) by DMSO with catalyst and heating [35]. The thiol (SH) group of an aminothiol (cysteine, $R-SH$) can be oxidized by potassium iodate in steps, successively, to a cysteine sulfenic acid derivative ($R-SOH$), a disulfide derivative (cystine, $R-S-S-R$), a cysteine sulfinic acid derivative ($R-SO_2H$), and finally, a sulfonic acid derivative (cysteic acid, $R-SO_3H$).

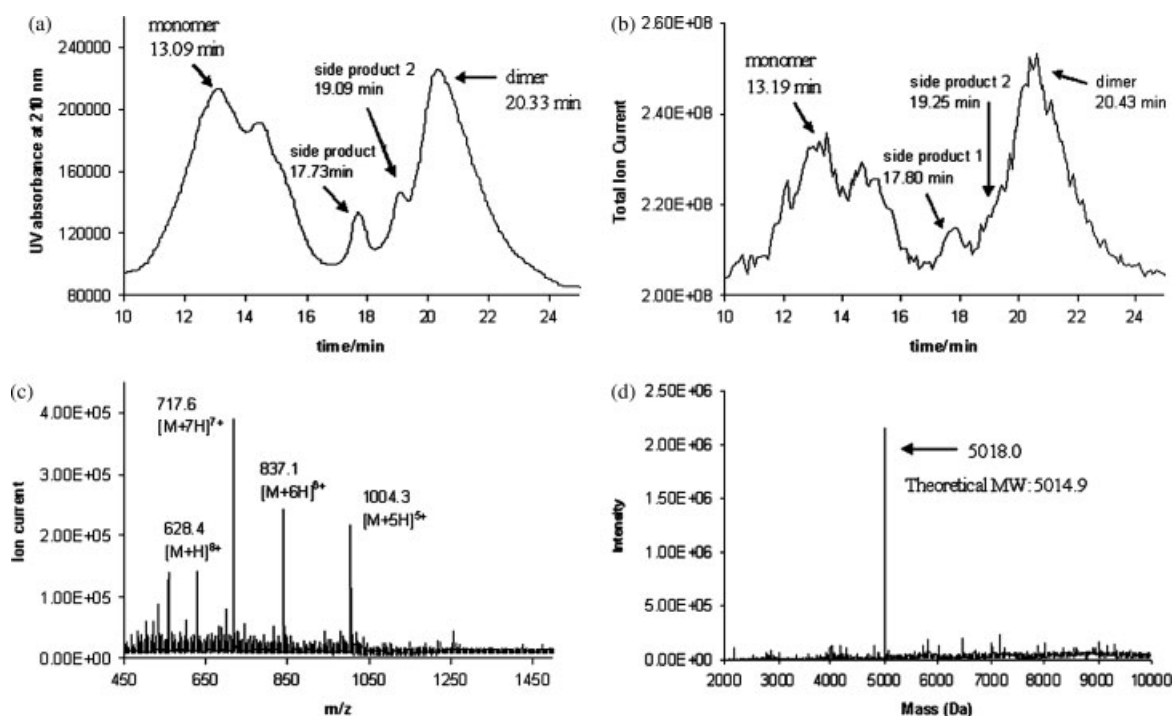


Figure 1. (a) UV chromatogram of C1A6 oxidation at 1 h. (b) Total ion current spectrum of C1A6 oxidation at 1 h. (c) ESI–MS analysis of C1A6 at 1 h. (d) Deconvoluted MS spectrum in ESI–MS analysis of C1A6 at 1 h. (e) ESI–MS analysis of C1A6-dimer at 1 h. (f) Deconvoluted MS spectrum in ESI–MS analysis of C1A6-dimer at 1 h. (g) ESI–MS analysis of side product 1 sulfenic acid ($RSOH$) at 1 h. (h) Deconvoluted MS spectrum in ESI–MS analysis of side product 1 at 1 h. (i) ESI–MS analysis side product 2 sulfinic acid (RSO_2H) at 1 h. (j) Deconvoluted MS spectrum in ESI–MS analysis of side product 2 at 1 h.

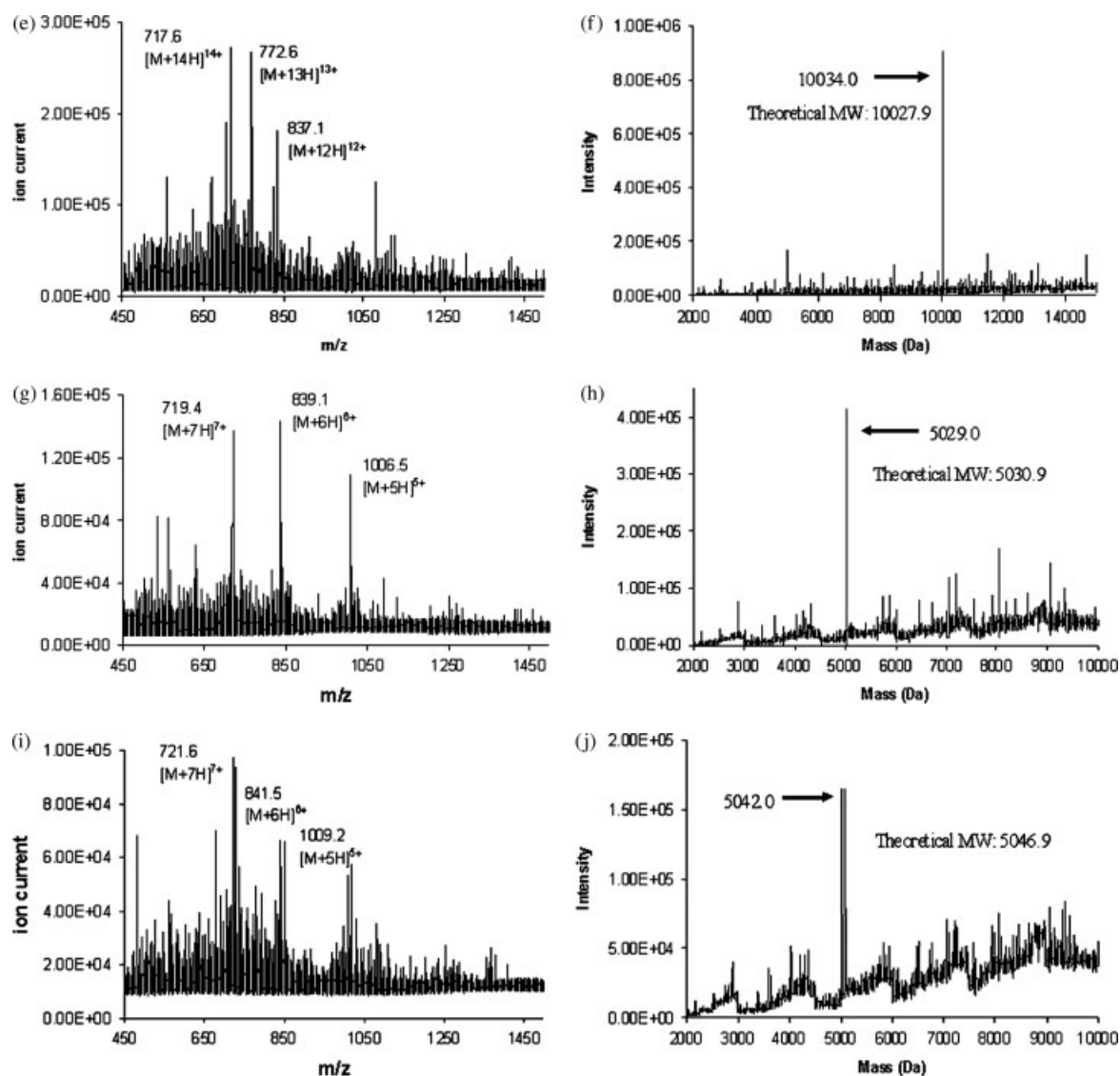


Figure 1. (Continued).

Consequently, oxidation of an aminothiols can yield one or more such products, depending on the reaction conditions, for example, the type of oxidized substrate, oxidation agents [21]. The oxidation products including two side products of three C1-peptides by DMSO (actually also by air, 0 h) are similar to those of thiols-containing small organic compounds reported elsewhere [21,35]. Our experimental data also show that oxidation agents (DMSO and air) can oxidize thiol group of cysteine to disulfide-linked products (e.g. 96%, 88% and 54% for C1A6-dimer, C1Y6-dimer and C1W6-dimer, respectively) and side products in their high oxidation states as minority (e.g. 4–12% of side product 1, <2% of side product 2). The amount of the C1-peptide-dimer decreases with increase of hydrophobicity of the C1-peptide monomer.

In general, DMSO can easily oxidize the thiol groups of *N*-terminus cysteine-containing analogues of hBD3 (the C1-peptides) to products of different oxidative states ranging from primary disulfide-linked dimers to higher oxidative states, such as sulfenic acid and sulfinic acid derivatives (see Eqns (1), (2) and (3)). In our experiments, the oxidizing agent is always in excess. Disulfide-

linked dimers were the major primary products, whereas the highly oxidized products of sulfenic acid and sulfonic acid derivatives were minor side products, but we did not find any sulfonic acid (*R*-SO₃H) derivatives. These products have different hydrophobicities and retention times, with the dimer always more hydrophobic than the other species (Table 2 and Figure 1(a), (b)); therefore, dimers can be easily separated from the oxidation mixtures. In general, the order for molecular hydrophobicity is as follows: the C1-peptide-dimer > sulfonic acid derivative (side product 2, <2%) > sulfenic acid derivative (side product 1) > the C1-peptide monomer; and this makes it easy to purify them by HPLC. Together these results suggest that DMSO is a suitable oxidizing agent for the preparation of intermolecular disulfide-linked homodimers of *N*-terminus cysteine-containing peptides (the C1-peptides).

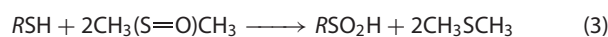
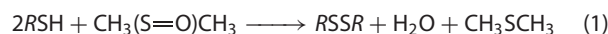


Table 4. The oxidation results of C1Y6 by DMSO (the first trial)

Oxidation time	Percentage of monomer	Percentage of dimer	Percentage of side product 1	Percentage of side product 2
0 h	92	0, but traces observed by MS	5	3
1 h	64	26	9	1
2 h	55	34	10	1
3 h	40	47	13	1
4 h	21	63	15	1
5 h	21	62	17	0
8 h	28	57	13	1
24 h	27	59	13	0
5 days	8	84	8	0

The oxidation concentration of peptide C1Y6 was 43.6 mg/ml, C1Y6 had partially been oxidized by air before addition of DMSO. At 1 h of oxidation, monomer *R*-SH (MW: 5567.5, theory; 5570.0, experiment); dimer *R*-S-S-*R*, (MW: 11133.0, theory; 1139.0, experiment); side product 1, sulfenic acid (*R*-SOH) (MW: 5583.5, theory; 5582.0, experiment); side product 2, sulfenic acid (*R*-SO₂H) (MW: 5599.5, theory; 5597.0, experiment).

Table 5. The oxidation results of C1W6 by DMSO

Oxidation time (h)	Percentage of monomer	Percentage of dimer	Percentage of side product 1	Percentage of side product 2
0	100	0	0, but traces observed by MS	0
1	93	4	2	0
2	89	8	3	0
3	84	13	3	0
4	79	16	4	0
24	75	15	11	2
48	41	54	4	0, but traces observed by MS

The oxidation concentration of C1W6 was 6.5 mg/ml, it was found that trace amount of C1W6 had been oxidized by air before addition of DMSO. At 48 h of oxidation, monomer *R*-SH (MW: 5705.7, theory; 5707.0, experiment); dimer *R*-S-S-*R* (MW: 11409.5, theory; 11414.0, experiment); side product 1, sulfenic acid (*R*-SOH) (MW: 5721.7, theory; 5720.0, experiment); side product 2, sulfenic acid (*R*-SO₂H) (MW: 5739.7, theory; 5733.0, experiment).

The Oxidation of the C29-peptides (C29A6, C29Y6 and C29W6) by DMSO

Table 6 shows that the oxidation of C29A6 proceeds very slowly in comparison with C1A6; and the yield of C29A6-dimer was 43% without any side products after 4 days of oxidation. For example, at 4 h, there was only 4% C29A6-dimer; in contrast, at 4 h, 91% of C1A6-dimer was formed. Again, after 4 days of oxidation, 43% of C29A6-dimer was observed with 57% of C29A6-monomer still remaining. On the contrary, C1A6 had been completely oxidized to dimer (96%) and the side product 1 (4%) between 8 and 24 h. Although the oxidation conditions including peptide and DMSO concentrations were similar, the molecular hydrophobicity of C29A6 is only a little larger than that of C1A6 (Tables 1 and 2). Given such similarities, it suggests that the large differences in oxidation rates of C1A6 and C29A6 may arise from structural factors such as: the participation of the conjunct group (NH₂) and the restricted accessibility of the SH group of C29A6 (see later). The data in Table 6 confirms that the SH of C29A6 are much less susceptible to oxidation to form a dimer than that of C1A6.

Effect of molecular hydrophobicity.

The oxidation results of C29Y6 and C29W6 (Table 2SI, Supporting Information) indicate that no corresponding dimers were observed even after 4 days of oxidation. It is clear that the oxidation of these two monomers is very slow indeed, even slower than that of C29A6. The reason for this trend could be attributed to the increase of

Table 6. The oxidation results of C29A6 by DMSO

Oxidation time	Percentage of monomer	Percentage of dimer
0 h	100	0
1 h	100	0, but traces observed by MS
2 h	100	0, but traces observed by MS
4 h	96	4
48 h	77	23
4 days	57	43

The oxidation concentration of monomer C29A6 was 3.1 mg/ml. After 4 days of oxidation, monomer C29A6 (*R*-SH) (MW: 4943.8, theory; 4945.0, experiment); dimer *R*-S-S-*R* (MW: 9885.7, theory; 9887.0, experiment).

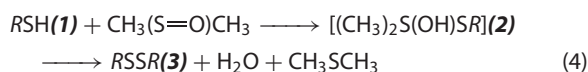
molecular hydrophobicity (C29W6 > C29Y6 > C29A6, Tables 1 and 2) which in turn will impinge on the folding of these peptides as seen in Figure 4.

The oxidation of C29A6, especially C29Y6 and C29W6 showed the inherent difficulties in obtaining large amounts of the C29-peptide-dimer; 43% C29A6-dimer had been formed even after 4 days of oxidation, whereas no C29Y6-dimer and C29W6-dimer were formed during the timescale of observation.

Mechanistic Interpretation of the Oxidation of *N*-terminus Cysteine-containing Analogues of hBD3: Effect of Conjoint Group (NH₂) Participation

Effect of conjoint group participation is a common concept in organic chemistry, often accelerating the rate of an organic reaction. It was clearly found that the three C1-peptides were easily oxidized to form their corresponding intermolecular disulfide-linked dimers as the major and primary products (96%, 84% and 54% for C1A6-dimer, C1Y6-dimer and C1W6-dimer, respectively) along with the highly oxidized side products sulfinic acid (side product 1 at 4%, 8% and 4%, respectively, for C1A6, C1Y6 and C1W6,) and sulfonic acid derivatives (side product 2, <2%) as minor products (Tables 3–5). The fast oxidation rates and the short times to total oxidation to form dimers of the C1-peptides in contrast to the C29-peptides could arise from the two structural parameters of the C1-peptides: the effect of conjoint group (NH₂) participation in oxidation and reduced steric hindrance to SH groups of C1-peptides in contrast to that in the C29-peptides. The effect of the conjoint group (NH₂) participation in oxidation can accelerate an oxidation reaction.

The general mechanism of disulfide formation by DMSO had been determined by Wallach and Mahon [36,37] and a simplified overall reaction is seen in Eqn (4).



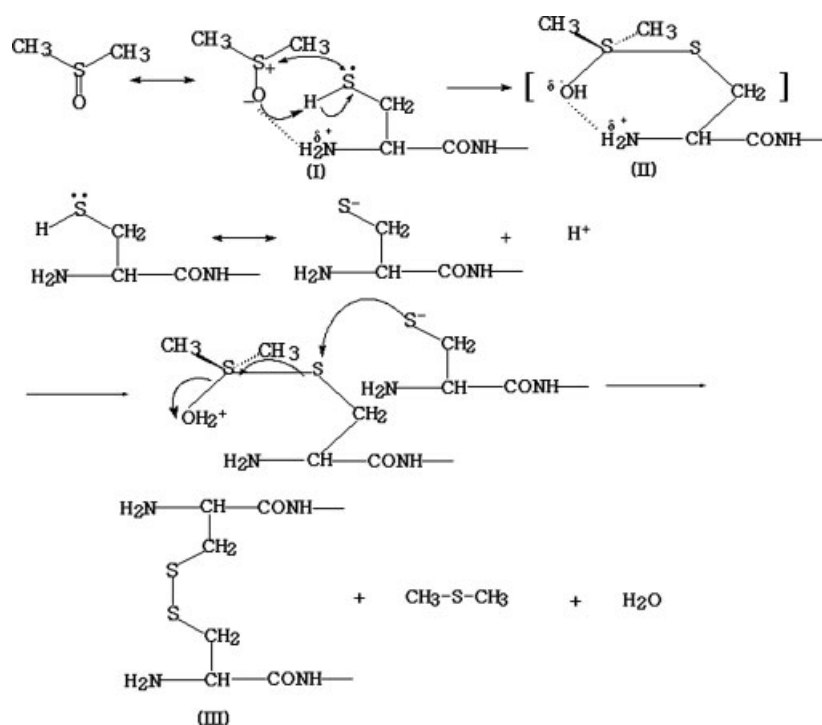
The reaction shows second-order kinetics and is strongly catalyzed by primary and secondary amines and somewhat weakly by acids. The rate determining step is the formation of an unstable adduct (**2**) that is rapidly captured by another thiol molecule (**1**) to yield the disulfide (**3**). Thus, the pH-independent rates between 3 and 8 can be rationalized by the overall kinetics [22]. The forward rate requires both the protonation of DMSO and formation of the

thiolate anion in the second step. The protonation favoured by the acidic pH is counterbalanced by a decrease in thiolate formation [22]. It is plausible that the rate acceleration of oxidation observed with C1-peptides containing a free amino terminal cysteine group (e.g. C1A6, C1Y6 and C1W6) is due to the assistance of the free amino group as a general base and its ability in the region-steering of DMSO to the thiol of the cysteine in the C1-peptides. Here, we propose that such regioselectivity is due to the weak interaction between the negative charge of the dipolar sulfoxide and the partially positive charge of the unprotonated amine in the C1-peptides that facilitated the formation of the unstable adducts (**I**) [22] followed by the formation of six-member cyclic intermediate (**II**), which is still unstable, but a little more stable than the adduct (**I**); the six-member cyclic intermediate is a common intermediate involved in organic reactions (Scheme 2). With the formation of the thiolate anion, a neutrophilic reaction subsequently occurs and an intermolecular disulfide bond (**III**) is formed. Such region-specific assistance and hence rate acceleration will not be possible in the oxidation of C29-peptides as they have only an amide and not an amino group.

The assistance of the free amino group as a general base, its ability in the region-steering of DMSO to the thiol of the cysteine in the C1-peptides and hence rate acceleration due to the effect of conjoint group (NH₂) participation in the oxidation reaction of the C1-peptides is shown in a proposed oxidation mechanism in Scheme 2.

Molecular Dynamics Simulations

Molecular dynamics simulations of the peptides were carried out to examine the folded structures of the peptides. The simulations were stable as judged from the evolution of the root mean squared deviations from the starting states and of the radii of gyration which show stable progressions (Figure 2(a), (b)). Starting from an



Scheme 2. The proposed oxidation mechanism of the C1-peptides by DMSO: effect of the conjoint group (NH₂) participation.

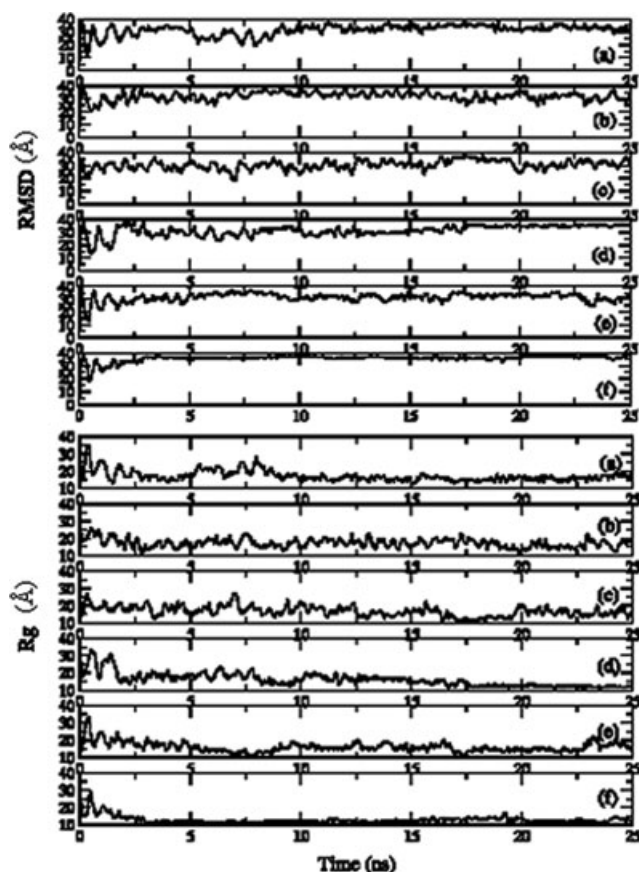


Figure 2. The time-dependant evolution of the root mean squared deviation and the radius of gyration of the peptides during the 25 ns of simulations for the C1-peptides containing Ala, Tyr and Trp are shown in (a), (c), (e), respectively, and in (b), (d), (f), respectively, for the corresponding C29 peptides.

extended state, we found that within 3 ns, all the systems had stabilized to an equilibrium state which is characterized by several interconverting conformers during the 25-ns sampled. During the process of oxidation of the peptides to yield the disulphide-linked dimer, the accessibility of the sulphur atoms of the cysteines will determine the rate of encounters with DMSO and subsequently with the other peptide molecules. We show this in Figure 3 and in Table 7. It is clear that the cysteine residues of the C29-peptides were unambiguously far less exposed than in the C1-peptides (Figure 3) and the same trend was displayed by the sulphur atoms of the cysteine residues. Thus, this marked difference in exposure makes the C29-peptides less able to interact with DMSO and thus provides a mechanistic rationale for their comparatively lower rates of oxidation. The exposed surfaces of the cysteines in the C1-peptides fluctuate between 150 and 200 Å² whereas that of the C29-peptides remain exposed less than 125 Å² (and sometimes 0, i.e. totally buried). The exposed surface of the 'S' atoms of the cysteines follows the same trend with an upper limit of ~75 Å² for the C1-peptides. The solvent accessible surface area (SASA) of the C29-peptides was lower because the cysteines were located in the middle of the peptides which were fairly hydrophobic overall. This places them in the centre of the region that would be globular as the peptides try to minimize their exposed hydrophobic surfaces in the aqueous environment and this would lead to the cysteine groups in the C29-peptides being well sequestered and thus not

Table 7. The accessible surface areas of the various peptides

Peptide	Time averaged SASA (Å ²)					cysteines sulphur atoms
	Total	Nonpolar	Polar	Nonpolar: polar	Cys	
C1A6	5267.0	3077.1	2190.9	1.40:1	186.5	67.8
C29A6	5463.0	3207.7	2255.4	1.42:1	85.7	37.8
C1Y6	5536.7	3247.4	2289.3	1.42:1	179.0	62.4
C29Y6	5105.7	2923.3	2182.3	1.34:1	22.1	12.5
C1W6	5177.9	3047.8	2130.1	1.43:1	181.8	66.3
C29W6	4946.5	2897.2	2049.3	1.41:1	86.6	37.2

accessible to solutes such as DMSO; we can see this in the three-dimensional structures of the peptides in snapshots taken at the end of the 25-ns simulations (Figure 4). In Figure 3, we also see that the accessibility of cysteine in C1W6 was the lowest of the C1-peptides, again accounting for the lowest rate of oxidation of C1W6 among the C1-peptides. Among all the peptides, we found that the cysteine in C29Y6 tends to be completely sequestered and hence buried. This peptide has eight Tyr side chains (in contrast to the other peptides that have only two Tyr residues: Y9, Y10). This results in a tendency for the Tyr side chains to cluster, thus completely sequestering the cysteine residue inside (Figure 4).

Conclusion

This study has examined the oxidation of SH groups of cysteine residues by DMSO leading to the formation of intermolecular disulphide-linked dimers in two series of linear analogues of hBD3 (*N*-terminus cysteine-containing linear peptides with cysteine at residue 1, the C1-peptides: C1A6, C1Y6 and C1W6; peptides with cysteine located at residue 29, the C29-peptides: C29A6, C29Y6 and C29W6). It was determined that the rate of oxidation, the formation and amount of products varied with the nature of the substrate, which included the location of the cysteine, the effect of conjunct group (NH₂) participation, molecular hydrophobicity, steric hindrance or the accessibility of the SH group and conformation.

The SH groups of C1-peptides, which have less steric hindrance, are more solvent exposed and have the assistance of the conjunct group (NH₂). These were generally susceptible to easy oxidation leading to the formation of dimers via an intermolecular disulfide link as a major product (92%, 84% and 54% for the three C1-peptide dimers), and additionally, two minor products: sulfenic acid (*R*-S-OH) (4–8%) and sulfinic acid (*R*-SO₂H) (0–2%) in highly oxidized states. The oxidation rate and amount of C1-peptide-dimers decreased with the increase in hydrophobicity of the C1-peptide. On the contrary, the SH groups of the C29-peptides with the cysteine located in the middle lack adjunct group participation are much less exposed to solvent, and hence are less susceptible and therefore slower to be oxidized to form dimers (e.g. 43% C29A6-dimer after 4 days of oxidation in the case of oxidation of C29A6 in contrast to 91% C1A6 at 4 h). In addition, the C29Y6-dimer and the C29W6-dimer are not observed even after 4 days of oxidation.

It appears from our data that high molecular hydrophobicity somehow makes the SH groups less accessible and hence renders them to slow oxidation to form dimers (or even fail to form

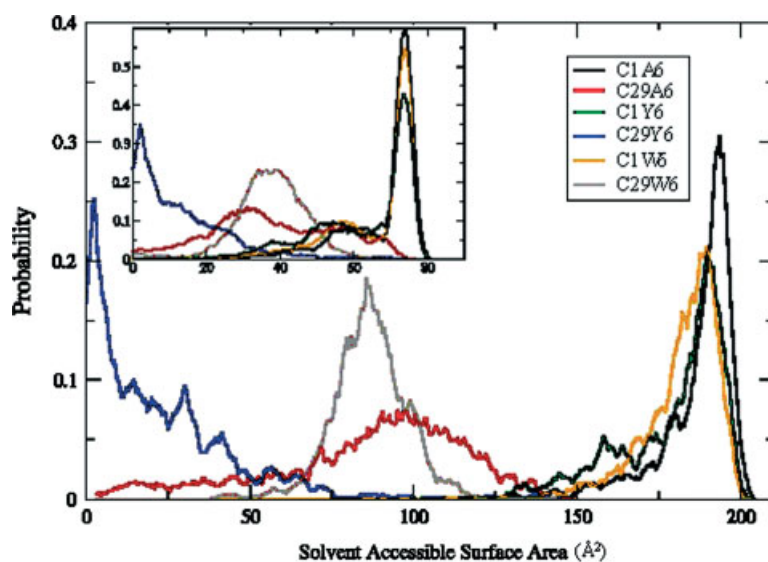


Figure 3. The density distribution of the accessible surface areas of the cysteine residues and those for the corresponding sulphur atoms (in inset) for the various peptides.

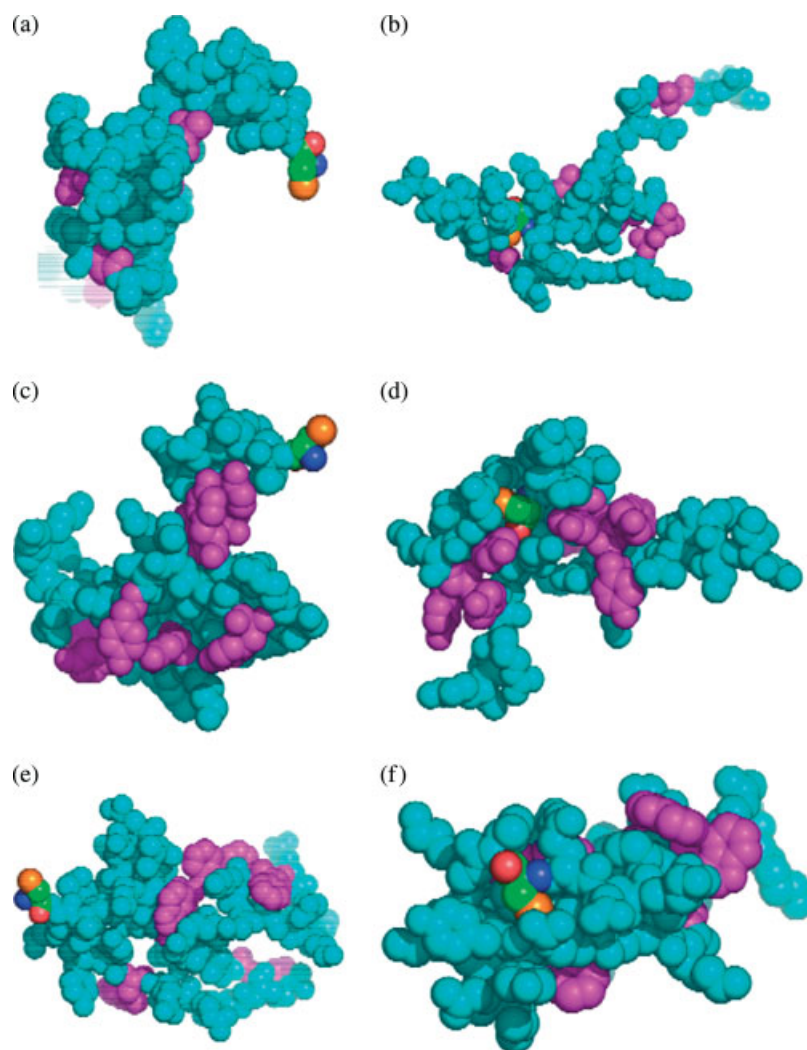


Figure 4. Snapshots of the conformation of the folded peptides at the end of 25 ns of molecular dynamics simulations for C1 [(a) Ala, (c) Tyr and (e) Trp] and C29 [(b) Ala, (d) Tyr and (f) Trp] peptides. The cysteine residue is shown in green, blue and red spheres with the sulphur atom shown in orange spheres. The sites of mutations Ala, Tyr and Trp are shown in magenta spheres. The rest of the peptide is shown in cyan spheres.

dimers during the timescale of observation). Molecular dynamics simulations have demonstrated that the exposure of the cysteines (and the sulphurs) of the C1-peptides was much larger than for the C29-peptides and that the larger hydrophobic side chains tend to cluster which sequesters the cysteines, particularly in the C29-peptides. Thus, a molecular explanation for the observed trends in oxidation rates may be suggested.

In conclusion, our findings enhance our understanding of the effects of the nature of the substrate peptides on the rate of oxidation by DMSO, the formation and amount of products (disulphide-linked dimeric peptides) and their purification. It also provides some understanding of the chemistry and biochemistry of thiol groups in peptides, proteins and enzymes and has biochemical implications due to the importance of the formation of intermolecular and intramolecular disulfide bonds in protein/enzyme and peptide chemistry.

Supporting information

Figures 1–6 for RP-HPLC–UV chromatograms and MS spectra of the six linear monomers of hBD3. Table 1SI and 2SI for the oxidation results of C1Y6 (the second trial), C29Y6 and C29W6.

Acknowledgements

The authors appreciate the support of the following grants from the National Medical Research Council of Singapore: NMRC/1106/2007, NMRC/0808/2003, NMRC/CPG/007/2004 and the NMRC-IBG. CV is adjunct at DBS (NUS), SBS (NTU) and NRF-TCR.

References

1. Powers JP, Hancock REW. The relationship between peptide structure and antibacterial activity. *Peptides* 2003; **24**(11): 1681–1691.
2. Cullor JS, Mannis MJ, Murphy CJ, Smith WL, Selsted ME, Reid TW. In vitro antimicrobial activity of defensins against ocular pathogens. *Arch. Ophthalmol.* 1990; **108**(6): 861–864.
3. McDermott AM, Redfern RL, Zhang B, Pei Y, Huang L, Proske RJ. Defensin expression by the cornea: multiple signalling pathways mediate IL-1 β stimulation of hBD-2 expression by human corneal epithelial cells. *Invest. Ophthalmol. Vis. Sci.* 2003; **44**(5): 1859–1865.
4. Zhou L, Huang LQ, Beuerman RW, Grigg ME, Li SF, Chew FT, Ang L, Stern ME, Tan D. Proteomic analysis of human tears: defensin expression after ocular surface surgery. *J. Proteome Res.* 2004; **3**: 410–416.
5. Li J, Raghunath M, Tan D, Lareu RR, Chen Z, Beuerman RW. Defensins HNP1 and HBD2 stimulation of wound-associated responses in human conjunctival fibroblasts. *Invest. Ophthalmol. Vis. Sci.* 2006; **47**: 3811–3819.
6. Dunsche A, Ail Y, Dommisch H, Siebert R, Schröder JM, Jepsen S. The novel human beta-defensin-3 is widely expressed in oral tissues. *Eur. J. Oral Sci.* 2002; **110**(2): 121–124.
7. Maisetta G, Batoni G, Esin S, Florio W, Bottai D, Favilli F, Campa M. In vitro bactericidal activity of human beta-defensin 3 against multidrug-resistant nosocomial strains. *Antimicrob. Agents Chemother.* 2006; **50**(2): 806–809.
8. Batoni G, Maisetta G, Esin S, Campa M. Human beta-defensin-3: a promising antimicrobial peptide. *Mini. Rev. Med. Chem.* 2006; **6**: 1063–1073.
9. Schibli DJ, Hunter HN, Aseyev V, Starner TD, Wiencek JM, McCray PB Jr, Tack BF, Vogel HJ. The solution structures of the human β defensins lead to a better understanding of the potent bactericidal activity of the HBD3 against *staphylococcus aureus*. *J. Biol. Chem.* 2002; **277**: 8279–8289.
10. Suresh A, Verma C. Modelling study of dimerization in mammalian defensins. *BMC Bioinformatics* 2006; **7**: S17.
11. Verma C, Seebah S, Low SM, Zhou L, Liu SP, Li J, Beuerman RW. Defensins: antimicrobial peptides for therapeutic development. *Biotechnol. J.* 2007; **2**(11): 1353–1359.
12. Campopiano DJ, Clarke DJ, Polfer NC, Barran PE, Langley RJ, Govan JR, Maxwell A, Dorin JR. Structure-activity relationships in defensin dimers, a novel link between β -defensin tertiary structure and antimicrobial activity. *J. Biol. Chem.* 2004; **279**: 48671–48679.
13. Hoover DM, Rajashankar KR, Blumenthal R, Puri A, Oppenheim JJ, Chertov O, Lubkowski J. The structure of human beta-defensin-2 shows evidence of higher order oligomerization. *J. Biol. Chem.* 2000; **275**: 32911–32918.
14. Gordon YJ, Romanowski EG, McDermott AM. A review of antimicrobial peptides and their therapeutic potential as anti-infective drugs. *Curr. Eye Res.* 2005; **30**: 505–515.
15. Hancock DM, Sahl HG. Antimicrobial and host-defense peptides as new anti-infective therapeutic strategies. *Nat. Biotechnol.* 2006; **24**: 1551–1557.
16. Ganz T. Fatal attraction evaded: how pathogenic bacteria resist cationic polypeptides. *J. Exp. Med.* 2001; **193**: F31–F34.
17. Wu Z, Hoover DM, Yang D, Boulegue C, Santamaria F, Oppenheim JJ, Lubkowski J, Lu W. Engineering disulfide bridges to dissect antimicrobial and chemotactic activities of human β -defensin 3. *Proc. Natl. Acad. Sci. U.S.A.* 2003; **100**: 8880–8885.
18. Hoover DM, Wu Z, Tucker K, Lu W, Lubkowski J. Antimicrobial characterization of human beta-defensin 3 derivatives. *Antimicrob. Agents Chemother.* 2003; **47**: 2804–2809.
19. Kluver E, Schulz-Maronde S, Scheid S, Meyer B, Forssmann WG, Adermann K. Structure-activity relation of human beta-defensin 3: influence of disulfide bonds and cysteine substitution on antimicrobial activity and cytotoxicity. *Biochemistry* 2005; **44**: 9804–9816.
20. Liu SP, Zhou L, Li J, Suresh A, Verma C, Foo YH, Yap E, Tan D, Beuerman R. Linear analogues of human beta-defensin 3: concepts for design of antimicrobial peptides with reduced cytotoxicity to mammalian cells. *ChemBioChem* 2008; **9**: 964–973.
21. For an extensive and earlier review of the course and mechanism of oxidation of biologically important SH groups see Friedman M. *The Chemistry and Biochemistry of the Sulfhydryl Group in Amino Acids, Peptides, and Proteins*. Pergamon Press: New York, 1973; Chapter 3.
22. Tam JP, Wu CR, Liu W, Zhang JW. Disulfide bond formation in peptides by dimethyl sulfoxide. Scope and applications. *J. Am. Chem. Soc.* 1991; **113**: 6657–6662.
23. Snow JT, Finley JW, Friedman M. Oxidation of sulfhydryl groups to disulfides by sulfoxides. *Biochem. Biophys. Res. Commun.* 1975; **64**: 441–447.
24. Duan Y, Wu C, Chowdhury S, Lee MC, Xiong G, Zhang W, Yang R, Cieplak P, Luo R, Lee T, Caldwell J, Wang J, Kollman P. A point-charge force field for molecular mechanics simulations of proteins based on condensed-phase quantum mechanical calculations. *J. Comput. Chem.* 2003; **24**: 1999–2012.
25. Onufriev A, Bashford D, Case DA. Modification of the generalized born model suitable for macromolecules. *J. Phys. Chem. B* 2000; **104**: 3712–3720.
26. Onufriev A, Case DA, Bashford D. Effective Born radii in the generalized Born approximation: the importance of being perfect. *J. Comput. Chem.* 2002; **23**: 1297–1304.
27. Ryckaert JP, Cicotti G, Berendsen HJC. Numerical-integration of Cartesian equations of motions of a system with constraints-molecular dynamics of n-alkanes. *J. Comput. Phys.* 1977; **23**: 327–341.
28. Berendsen HJC, Postma JPM, Van Gunsteren WF, Dinola A, Haak JR. Molecular dynamics with coupling to an external bath. *J. Chem. Phys.* 1984; **81**: 3684–3690.
29. Blondelle SE, Houghten RA. Design of model amphipathic peptides having potent antimicrobial activities. *Biochemistry* 1992; **31**: 12688–12694.
30. Raguse TL, Porter EA, Weisblum B, Gellman SH. Structure-activity studies of 14-helical antimicrobial beta-peptides: probing the relationship between conformational stability and antimicrobial potency. *J. Am. Chem. Soc.* 2002; **124**: 12774–12785.
31. Schmitt MA, Weisblum B, Gellman SH. Interplay among folding, sequence and lipophilicity in the antibacterial and hemolytic activities of alpha/beta-Peptides. *J. Am. Chem. Soc.* 2007; **129**: 417–428.
32. Kim S, Kim SS, Lee BJ. Correlation between the activities of alpha-helical antimicrobial peptides and hydrophobicities

- represented as RP HPLC retention times. *Peptides* 2005; **26**: 2050–2056.
33. Hodges RS, Chen Y, Kopecky E, Mant CT. Monitoring the hydrophilicity/hydrophobicity of amino acid side-chains in the non-polar and polar faces of amphipathic alpha-helices by reversed-phase and hydrophilic interaction/cation-exchange chromatography. *J. Chromatogr., A* 2004; **1053**: 161–172.
 34. Hopp TP, Woods KR. Prediction of protein antigenic determinants from amino acid sequences. *Proc. Natl. Acad. Sci. U.S.A.* 1981; **78**: 3824–3828.
 35. Lowe OG. Oxidation of thiols and disulfides to sulfonic acids by dimethyl sulfoxide. *J. Org. Chem.* 1976; **41**: 2061–2064.
 36. Wallace TJ. Reactions of thiols with sulfoxides. I. Scope of the reaction and synthetic applications. *J. Am. Chem. Soc.* 1964; **86**: 2018–2021.
 37. Wallace TJ, Mahon JJ. Reactions of thiols with sulfoxides. II. Kinetics and mechanistic implications. *J. Am. Chem. Soc.* 1964; **86**: 4099–4103.